

PhysVideo: Physically Plausible Video Generation with Cross-View Geometry Guidance

Cong Wang^{*1,2} Hanxin Zhu^{*3} Xiao Tang⁴ Jiayi Luo⁵ Xin Jin⁶ Long Chen^{†1} Fei-Yue Wang¹
Zhibo Chen^{†2,3}

Abstract

Recent progress in video generation has led to substantial improvements in visual fidelity, yet ensuring physically consistent motion remains a fundamental challenge. Intuitively, this limitation can be attributed to the fact that real-world object motion unfolds in three-dimensional space, while video observations provide only partial, view-dependent projections of such dynamics. To address these issues, we propose **PhysVideo**, a two-stage framework that first generates physics-aware orthogonal foreground videos and then synthesizes full videos with background. In the first stage, **Phys4View** leverages physics-aware attention to capture the influence of physical attributes on motion dynamics, and enhances spatio-temporal consistency by incorporating geometry-enhanced cross-view attention and temporal attention. In the second stage, **VideoSyn** uses the generated foreground videos as guidance and learns the interactions between foreground dynamics and background context for controllable video synthesis. To support training, we construct **PhysMV**, a dataset containing 40K scenes, each consisting of four orthogonal viewpoints, resulting in a total of 160K video sequences. Extensive experiments demonstrate that PhysVideo significantly improves physical realism and spatio-temporal coherence over existing video generation methods. Home page: <https://anonymous.4open.science/w/Phys4D/>.

¹the State Key Laboratory of Multimodal Artificial Intelligence Systems, Institute of Automation, Chinese Academy of Sciences. ²Zhongguancun Academy ³School of Information Science and Technology, University of Science and Technology of China ⁴College of Automotive and Energy Engineering, Tongji University ⁵SKLCCSE, School of Computer Science and Engineering, Beihang University ⁶Eastern Institute of Technology. Correspondence to: Long Chen <long.chen@ia.ac.cn>, Zhibo Chen <chenzhibo@ustc.edu.cn>.

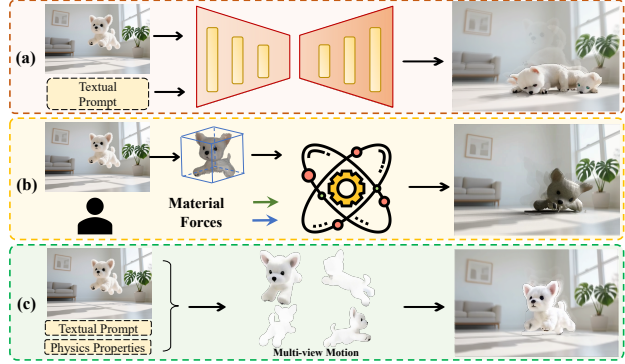


Figure 1. Comparison of our method with prior video generation paradigms. (a) Data-driven generative models. (b) Physics-engine-based methods. (c) Our physics-aware two-stage framework utilizing foreground multi-view videos.

1. Introduction

Recent advances in video generation have significantly expanded the capability of visual synthesis models, enabling the generation of high-fidelity and temporally coherent videos conditioned on multimodal inputs such as text and images (Blattmann et al., 2023; Zheng et al., 2024; Kong et al., 2024; Yang et al., 2025b; Wan et al., 2025). In particular, text- and image-conditioned video generation (TI2V) has emerged as a powerful paradigm for synthesizing dynamic visual content that aligns semantic intent with visual appearance. As perceptual quality improves, these models are increasingly seen as a foundation for interactive content creation, simulation-based reasoning, and embodied AI in dynamic visual environments.

Despite this progress, current video generation models still struggle to produce physically plausible and spatially consistent motion (Bansal et al., 2024; Meng et al., 2024). While visually convincing at the pixel level, generated videos often violate basic physical principles, exhibiting implausible accelerations, inconsistent object interactions, or motion patterns that are insensitive to intrinsic object properties such as mass or elasticity, as shown in Fig. 1.(a). These issues become particularly evident in background-aware synthesis, where realistic interactions between moving foreground objects and the surrounding scene are essential.

We attribute these limitations to a mismatch between pixel-

space motion modeling and physically constrained motion. Existing video generators typically learn dynamics as appearance transformations across frames, yet physically plausible motion and deformation are governed by geometry and material properties and should remain consistent across viewpoints. Explicit 3D representations and physics-based simulation (Xie et al., 2024; Lin et al., 2025a; Liu et al., 2024a) can produce valid trajectories, but they often rely on multi-stage pipelines that are difficult to scale and hard to integrate into end-to-end training, and they can hinder efficient feed-forward generation under flexible multimodal conditioning. Instead, we consider a setting that directly outputs synchronized multi-view foreground motion (e.g., four viewpoints) conditioned on physical attributes, and evaluates physical realism through both input-consistency with the specified physical properties and cross-view consistency, without explicitly outputting 3D structure or performing explicit 3D modeling.

In this work, we take a foreground-first view of physically grounded motion: we generate synchronized multi-view foreground dynamics under explicit physical attributes, and then use them to guide final video synthesis. Building on this idea, we propose **PhysVideo**, a physics-driven framework that enables geometry-aware motion modeling for video generation without explicitly reconstructing 3D geometry. PhysVideo adopts a two-stage design. In the first stage, **Phys4View** generates multi-view foreground motion conditioned on a single image, a textual prompt, and explicit physical attributes. By injecting physical parameters directly into the attention mechanism and conditioning on control videos constructed from foreground masks and multi-view priors, Phys4View incorporates physical and geometric cues into motion generation. We further introduce a geometry-aware cross-view attention module together with temporal attention to enhance cross-view alignment and spatiotemporal coherence, enabling simultaneous generation of synchronized four-view videos. In the second stage, **VideoSyn** synthesizes background-aware image-to-video results by leveraging the generated multi-view motion as guidance, allowing the model to learn data-driven foreground-background interactions such as contact, occlusion, and context-consistent motion. To support training of the four-view video generation model, we employ a physics engine together with 3D-GS object representations to construct a physics-driven multi-view dataset, PhysMV, which comprises 10K 3D objects and 40K orthogonal video sets, totaling 160K videos.

Our contributions can be summarized as follows:

- We introduce **PhysVideo**, a feed-forward framework for physics-driven, geometry-aware motion modeling in video generation, conditioned on images, text, and explicit physical attributes.
- We propose **Phys4View**, which integrates physics-aware

attention with spatiotemporal and cross-view modeling to generate temporally coherent and geometrically consistent multi-view motion.

- We develop **VideoSyn** for background-aware image-to-video synthesis, where multi-view motion guidance enables data-driven learning of realistic foreground-background interactions without explicit physical simulation at inference.
- We construct a large-scale physics-oriented multi-view video dataset using a physics engine. We further show that PhysVideo, leveraging multi-view foreground motion generation followed by motion-aware video synthesis, achieves superior physical realism, temporal coherence, and cross-view consistency compared to prior video generation methods.

2. Related Works

2.1. Controllable Video Generation

Video generation models trained on large-scale text-video paired datasets have demonstrated remarkable capabilities in synthesizing high-quality videos (Ho et al., 2022; Blattmann et al., 2023; Kong et al., 2024; Yang et al., 2025b). Previous studies have shown that pretrained models can be additionally guided by various control signals, including camera motion (Fu et al., 2024; He et al., 2024), point trajectories (Geng et al., 2025; Gu et al., 2025; Burgert et al., 2025), and anchor-frame videos (Chen et al., 2025b; Romero et al., 2025), enabling more controllable video generation. Meanwhile, other research efforts have explored leveraging different modalities to guide motion-aware video synthesis. Some approaches (Li et al., 2024; Jin et al., 2025) employ optical flow videos as guidance, using flow maps to characterize motion dynamics and subsequently synthesize RGB videos based on them. Other methods (Liang et al., 2024; Lv et al., 2024) use depth videos as conditioning inputs to guide the generation of temporally coherent video sequences. In addition, several text-driven approaches (Xue et al., 2025) attempt to infer more fine-grained descriptions of motion dynamics from textual instructions, thereby enabling more precise control over motion behaviors during video generation. However, these methods generally lack the modeling of physical laws and often produce results that violate basic principles of physical plausibility. To address this limitation, our method generates physics-aware multi-view videos as motion representations and subsequently renders them into plausible video outputs.

2.2. Physics-grounded Video Generation

Physics engines typically use the 3D representation of foreground objects as input to simulate and generate the 3D state at each time step, based on defined material and motion

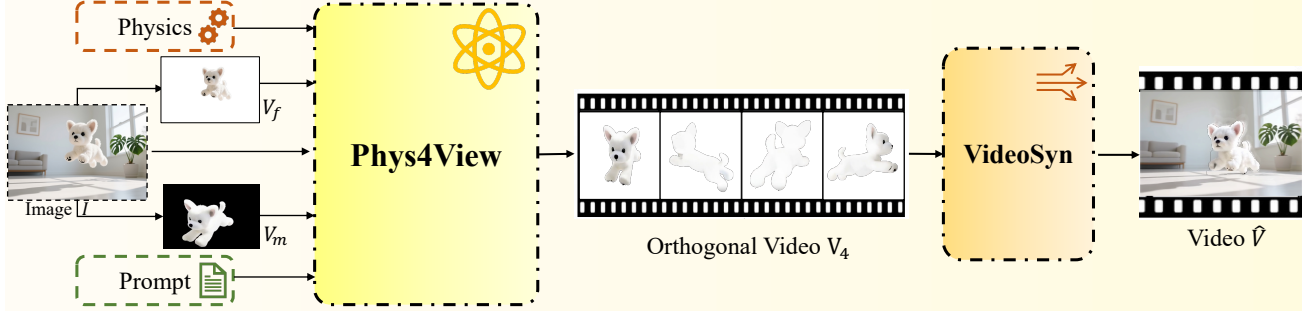


Figure 2. **Pipeline of PhysVideo.** PhysVideo generates physically plausible videos via a two-stage pipeline: 1) generating physics-aware orthogonal foreground videos, 2) generating a plausible video with the guidance of foreground motion.

properties (Xie et al., 2024; Chen et al., 2025a). Leveraging the renderable 3D-GS representation (Kerbl et al., 2023), some methods (Xie et al., 2024) propose using the Material Point Method (MPM) solver to update the 3D Gaussian representation at each time step after force-induced motion. However, due to the limitations of MPM, it is only suitable for simulating elastic objects. To address the shortcomings of MPM solvers, some approaches (Feng et al., 2024; Gao et al., 2025) incorporate Position-Based Dynamics (PBD) solvers to simulate fluid motion. The use of physics engines requires additional definition of physical properties, and some methods (Zhao et al., 2025; Mao et al., 2025) propose using MLLMs to estimate properties such as Young’s modulus, Poisson’s ratio, and density. Furthermore, other methods (Huang et al., 2025; Lin et al., 2025b; Zhang et al., 2024) suggest utilizing the prior knowledge of pre-trained video generation models to iteratively optimize the material properties of objects through SDS loss (Poole et al., 2022) after rendering the video. Although physics-engine-based methods ensure physical plausibility, they require manual definition of simulation conditions such as material properties and external forces and depend on high-quality explicit 3D representations, limiting their ability to automatically generate high-quality videos from a single image.

3. Methodology

We propose a two-stage generation framework that first produces orthogonal videos with physically grounded motion and subsequently synthesizes visually realistic videos with foreground–background interactions, as shown in Fig. 2. The orthogonal video generation model, **Phys4View**, is presented in Sec. 3.1 and Sec. 3.2, followed by the video synthesis model, **VideoSyn**, in Sec. 3.3.

3.1. Physics Conditioning and Video Prior Fusion

Phys4View aims to generate temporally coherent and geometrically consistent orthogonal videos conditioned on a single image I , a textual prompt T , and physical attributes P . Given an input image containing both foreground and background regions, we first extract a foreground object

mask M_f using a semantic segmentation model (Ren et al., 2024b). Based on M_f , we isolate the foreground image I_f and construct a foreground-initialized video V_f by replicating I_f across the temporal dimension. To provide 3D structural priors for subsequent video generation, we further employ a pretrained image-to-3D generation model (Xiang et al., 2025) to obtain a static multi-view video V_m , which serves as geometric guidance.

Video prior conditioning. We condition video generation on two complementary video priors: a foreground-initialized video V_f and a multi-view structural prior V_m . Both priors are encoded into latent features H_f and H_m , and are adaptively fused via a lightweight gating mechanism. Specifically, we predict a gating tensor from their concatenation and compute the fused representation as

$$H_v = G \odot H_f + (1 - G) \odot H_m, \quad (1)$$

where $G = \text{Proj}(H_f \oplus H_m)$ and $\text{Proj}(\cdot)$ is a lightweight 3D convolutional projector. We then inject H_v into the intermediate hidden representation H_i by replacing a designated subset of channels:

$$H_c = \text{Inject}(H_i, H_v). \quad (2)$$

Physical and semantic conditioning. We condition generation on object-level physical attributes, including motion cues (e.g., acceleration \mathbf{a} and velocity \mathbf{v}) and material properties (e.g., density ρ , Young’s modulus E , and Poisson’s ratio ν). To avoid semantic distortion from an expressive attribute encoder, we adopt a parameter-free tokenization scheme and obtain a unified physical conditioning token sequence C_{phys} .

We incorporate C_{phys} into the generator via a physics-aware attention module that modulates the intermediate representation H_c :

$$H_{\text{phys}} = H_c + \alpha_{\text{phys}} \cdot \text{Attn}_{\text{phys}}([H_c; C_{\text{phys}}]), \quad (3)$$

where α_{phys} is a learnable scaling factor. For textual conditioning, we follow the standard text cross-attention used in

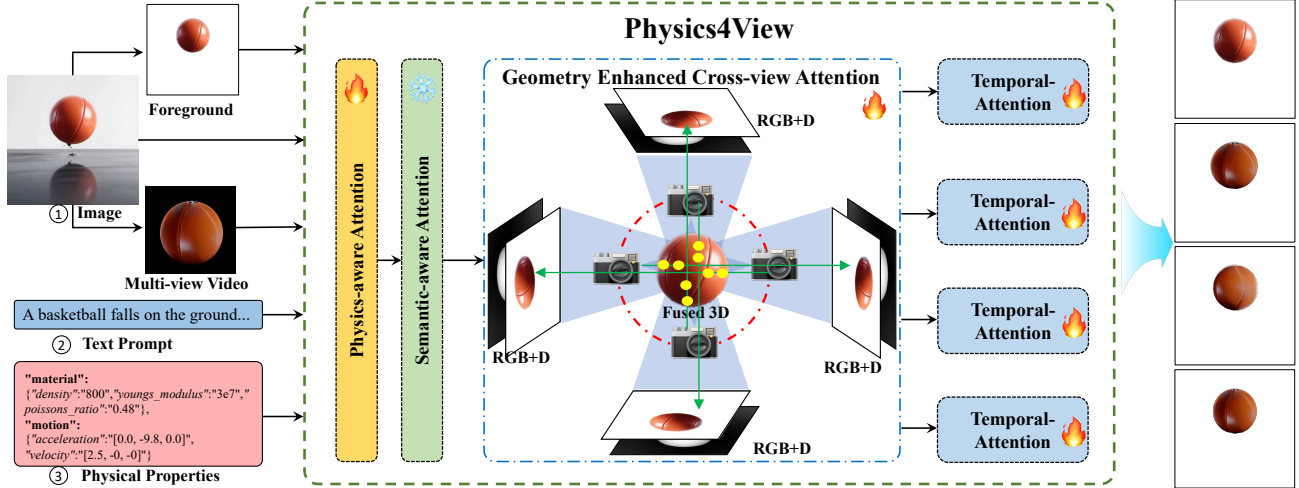


Figure 3. **Overview of Phys4View.** The framework incorporates physics-aware attention to model physical motion and introduces a geometry-enhanced cross-view attention module to generate spatially and temporally consistent orthogonal videos.

the pretrained TI2V model (Yang et al., 2025b):

$$H = H_{\text{phys}} + \alpha_t \cdot \text{Attn}_t(H_{\text{phys}}; C_p), \quad (4)$$

where C_p denotes the encoded prompt.

3.2. Geometry-enhanced Cross-view and Temporal Attention

To prove spatial and temporal consistency, we introduce a geometry-enhanced cross-view and temporal attention, as illustrated in Fig. 3.

Camera pose fusion. Before applying spatiotemporal attention, we inject camera pose information into the four-view latent features in a lightweight manner. Specifically, we encode the per-view camera pose into a learnable embedding, concatenate it with the corresponding latent along the channel dimension, and use a small convolutional block to fuse them, yielding pose-aware features for subsequent cross-view interaction.

Geometry-enhanced cross-view attention. To encourage spatially coherent cross-view interactions while avoiding explicit 3D representation, we introduce a geometry-guided bias into the cross-view attention mechanism based on predicted depth.

Given the latent feature map H , we predict a dense depth map at the same spatial resolution:

$$D = \mathcal{P}_\theta(H), \quad (5)$$

where \mathcal{P}_θ denotes a learnable depth prediction head. Each spatial location i in the latent grid, associated with coordinates (u_i, v_i) , is lifted into the camera coordinate system via

$$\mathbf{x}_i^{\text{cam}} = D_i \mathbf{K}^{-1} \begin{bmatrix} u_i \\ v_i \\ 1 \end{bmatrix}, \quad (6)$$

where \mathbf{K} is the camera intrinsic matrix.

Using the reconstructed 3D points in camera coordinates, we compute the pairwise geometric distance between locations i and j as

$$d_{ij} = \|\mathbf{x}_i^{\text{cam}} - \mathbf{x}_j^{\text{cam}}\|_2. \quad (7)$$

This distance is converted into a geometry-based affinity weight:

$$w_{ij,d} = \exp\left(-\frac{d_{ij}^2}{\tau}\right), \quad (8)$$

where τ controls the spatial sensitivity of the geometric prior.

Since depth prediction may be unreliable near occlusion boundaries or textureless regions, we further introduce a depth-confidence term to downweight ambiguous correspondences. Specifically, we define:

$$w_{ij,\text{conf}} = \alpha + (1 - \alpha) \left(1 - f_\theta\left(\frac{\|\nabla D_i\|_2 + \|\nabla D_j\|_2}{|D_i| + |D_j| + \epsilon}\right)\right), \quad (9)$$

where ∇D_i denotes the local spatial depth gradient at location i , $f_\theta(\cdot)$ is a learnable confidence mapping function, ϵ is a small constant for numerical stability, and α provides a lower bound on the confidence weight.

The final geometry-aware affinity between locations i and j is given by:

$$w_{ij} = w_{ij,d} \cdot w_{ij,\text{conf}}. \quad (10)$$

We incorporate this geometric prior into cross-view attention by augmenting the attention logits as:

$$s_{ij}^{\text{geo}} = \frac{Q_i \cdot K_j}{\sqrt{d}} + \log(w_{ij}), \quad (11)$$

where Q_i and K_j denote the query and key features at locations i and j , respectively. This formulation softly biases

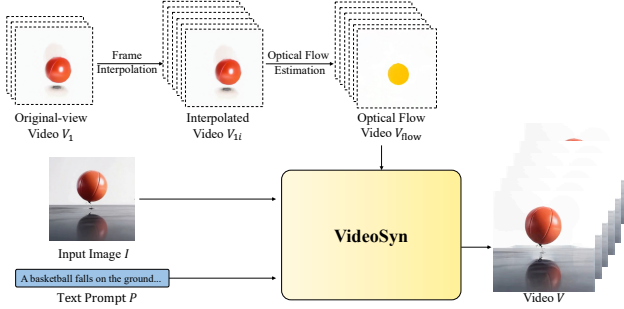


Figure 4. **Overview of VideoSyn.** The framework extracts foreground motion cues from a pre-generated physics-aware video and leverages them to guide the full video generation process.

the attention mechanism toward spatially compatible and geometrically plausible regions under the predicted depth, while suppressing unreliable interactions.

Temporal attention. To further enhance temporal consistency in the generated videos, we introduce a lightweight temporal attention mechanism. Given the feature representation H , we first partition it into four disjoint components along the channel dimension as $H = [H_1; H_2; H_3; H_4]$, where $[\cdot; \cdot]$ denotes channel-wise concatenation.

For each component H_i , we apply an independent temporal self-attention operation to model temporal dependencies:

$$H'_i = H_i + \alpha_t \cdot \text{Attn}(H_i), \quad (12)$$

where $\text{Attn}(\cdot)$ denotes the temporal attention module and α_t is a learnable scaling factor that controls the strength of temporal aggregation.

Finally, the temporally enhanced features from all groups are concatenated to form the final representation $H_{\text{final}} = [H'_1; H'_2; H'_3; H'_4]$.

3.3. Motion-guided Plausible Video Generation

After obtaining a physics-aware four-view video V_4 , our goal is to synthesize a visually coherent RGB video that captures realistic foreground-background interactions. To this end, we first extract the original-view video V_1 from V_4 . We then apply a frame interpolation model (Wu et al., 2024) to densify the temporal resolution by interpolating four intermediate frames between consecutive frames, resulting in an extended video sequence V_{1i} .

To explicitly leverage the motion information encoded in V_{1i} as guidance for video generation, we adopt optical flow as a motion control signal. Specifically, we employ a pre-trained optical flow estimation model (Dong & Fu, 2024) to compute the corresponding flow video V_{flow} from V_{1i} . The resulting optical flow captures fine-grained motion dynamics while remaining agnostic to appearance variations, making it a suitable representation for motion conditioning.

We then incorporate V_{flow} as an explicit motion control condition in the video generation process:

$$\tilde{V} = \text{Attn}([H; H_{\text{flow}}; C_p]), \quad (13)$$

where H_{flow} is the encoded latent of the optical flow video V_{flow} . The attention module integrates appearance, motion, and semantic guidance for prediction.

The final video latent \hat{V} is obtained through the diffusion denoising process:

$$\hat{V} = \mathcal{D}_\theta(\tilde{V}_t, t), \quad (14)$$

where \tilde{V}_t denotes the noisy latent sampled at diffusion timestep t .

3.4. Training

PhysMV dataset. To facilitate the training of our physics-aware, multi-view video generation model, we construct PhysMV, a large-scale dataset comprising 40K distinct motion sequences, each captured from four orthogonal view-points, resulting in a total of 160K single-view videos. Existing physics-engine-based video datasets predominantly focus on synthesizing single-view dynamic videos. In contrast, PhysMV generates orthogonal videos simultaneously while maintaining physically grounded simulations, enabling explicit multi-view geometric supervision. To build up the dataset, we generate 10K foreground objects represented as 3D Gaussian Splatting (3D-GS) models using Trellis (Xiang et al., 2025). Additional dataset details are provided in Appendix C.

Phys4View training. We train the proposed Phys4View model using a standard diffusion objective. Specifically, the base training loss is defined as

$$\mathcal{L}_{\text{base}} = \mathbb{E}_{\tilde{F}_t, t} \left[w_1(t) \|\mathcal{D}_\theta(\tilde{F}_t, t) - \bar{F}\|_2^2 \right], \quad (15)$$

where \tilde{F}_t denotes the noisy latent at diffusion timestep t , \bar{F} is the target latent, and $w_1(t)$ is a timestep-dependent weighting function.

To provide geometric supervision, we additionally impose a depth consistency loss using relative depth estimates. Given the predicted depth map D and the estimated relative depth D_r , we define the depth supervision loss as

$$\mathcal{L}_{\text{depth}} = \left\| \frac{\text{Cov}(D, D_r)}{\sqrt{\text{Var}(D) \text{Var}(D_r)}} \right\|_1, \quad (16)$$

which measures the scale-invariant correlation between the predicted and reference depth maps.

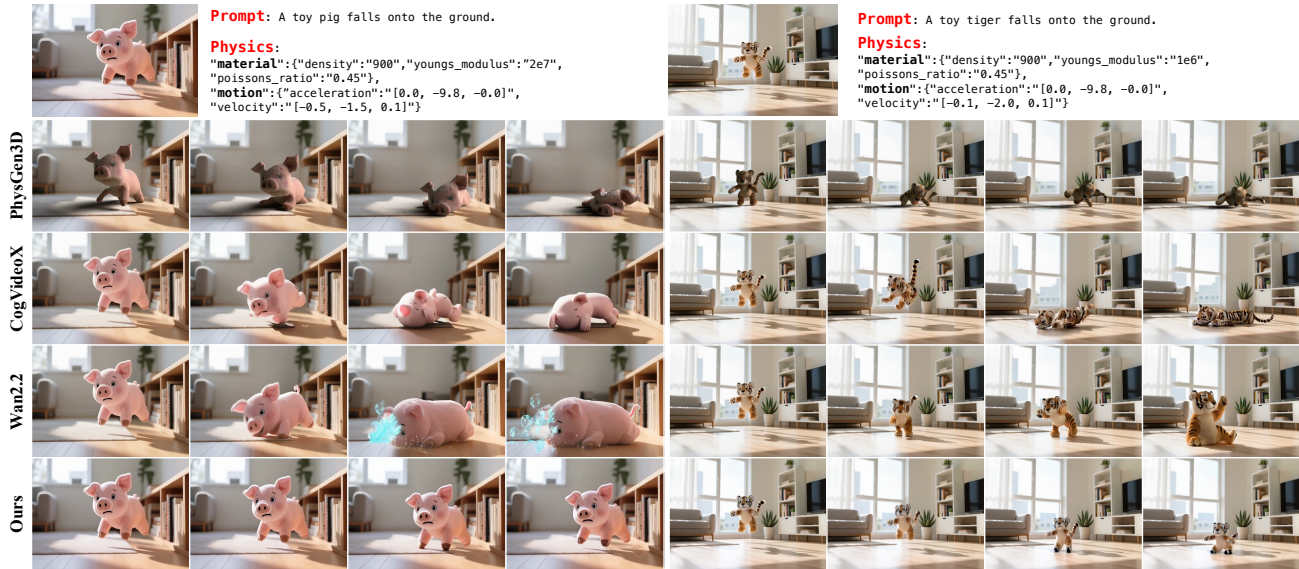


Figure 5. **Qualitative comparisons.** The top row shows the given image, text prompt and corresponding physics settings. For the definition of velocity and acceleration directions, the positive x-axis is defined as horizontal left, the positive y-axis as vertical upward, and the positive z-axis as perpendicular to the paper plane inward.

VideoSyn training. To train VideoSyn, we adopt a diffusion-based image-to-video learning paradigm in which the model learns to generate a video conditioned on the motion guidance from the original view. We preprocess the OpenVid (Nan et al., 2024) and WISA (Wang et al., 2025) datasets and train the VideoSyn model on both datasets. During training, we minimize the mean squared error between the denoised prediction and the ground-truth frame under random diffusion steps:

$$\mathcal{L}_2 = \mathbb{E}_{\tilde{R}_t, t} \left[w_2(t) \left\| \mathcal{D}_\theta(\tilde{R}_t, t) - \bar{R} \right\|_2^2 \right], \quad (17)$$

where \bar{R} is the ground-truth RGB video. This training objective guides VideoSyn to synthesize temporally coherent and visually realistic video sequences that faithfully follow the motion guidance.

4. Experiments

4.1. Experimental Setups

Implementation details. Our model is trained on 8 NVIDIA A100 GPUs, each with 80GB of memory, while all inference experiments are performed on a single A100 GPU. To assess the effectiveness of the proposed approach, we construct a benchmark dataset consisting of 33 test samples. Each sample comprises a single RGB image I with a resolution of 720×480 , an associated textual prompt P , and object-level physical attributes generated by GPT-4o. The benchmark set includes both rigid and deformable objects to evaluate the model’s generalization across diverse physical regimes. All input images are synthesized in a photorealistic style using a text-to-image generation model (Wu

et al., 2025). For each input image, we obtain the foreground object mask M_f using Grounded-SAM (Ren et al., 2024b). Based on the extracted foreground, we further generate multi-view videos and corresponding 3D Gaussian Splatting (3D-GS) representations with Trellis (Xiang et al., 2025), which are used for downstream evaluation.

Baselines. We compare the proposed method with two categories of baselines: physics-engine-based approaches and learning-based video generation models. For the physics-engine-based category, we include representative methods such as PhysGen (Liu et al., 2024b), PhysGen3D (Chen et al., 2025a), and OmniPhysGS (Lin et al., 2025b). These methods explicitly rely on physical simulation to model object dynamics and serve as strong references for physics-grounded video generation. We also evaluate against state-of-the-art video generation models, including general-purpose frameworks such as CogVideoX (Yang et al., 2025b) and Wan (Wan et al., 2025). In addition, we consider Force Prompting (Gillman et al., 2025), a recent method that enhances video generation with explicit physical priors.

Metrics. We evaluate the quality of the generated videos using a combination of automatic metrics and VLM-based assessments. Specifically, WorldScore (Duan et al., 2025) is used to quantify photometric consistency (Photo), multi-view geometric consistency (3D Consist), and motion smoothness (Motion). Complementarily, we employ VBench (Huang et al., 2024) to assess motion quality (Motion), subject consistency (Subject), temporal flickering (Flickering), and overall visual fidelity (Image). To further measure adherence to the input prompts, following the evaluation protocol of PhysGen3D (Chen et al., 2025a), we

Table 1. Quantitative comparisons on WorldScore and VBench. **Bold**: Best. Underline: Second Best.

Method	WorldScore			VBench			
	Photo \uparrow	Motion \uparrow	3D Consist \uparrow	Motion \uparrow	Subject \uparrow	Flickering \uparrow	Image \uparrow
CogVideoX-I2V-5B (Yang et al., 2025b)	64.72	67.39	74.43	0.993	0.886	0.989	0.636
Wan2.2-TI2V-5B (Wan et al., 2025)	65.97	64.90	63.86	0.994	0.926	0.991	<u>0.653</u>
Force Prompting (Gillman et al., 2025)	74.38	72.53	50.97	0.994	0.938	0.992	0.641
OmniPhysGS (Lin et al., 2025b)	58.67	<u>90.65</u>	37.24	0.995	0.929	0.995	0.378
PhysGen (Liu et al., 2024b)	<u>90.80</u>	82.45	84.27	0.995	<u>0.956</u>	0.994	0.648
PhysGen3D (Chen et al., 2025a)	86.68	86.34	<u>86.89</u>	<u>0.996</u>	0.910	0.998	0.605
Ours	94.09	93.62	87.19	0.996	0.970	<u>0.996</u>	0.655

Table 2. GPT-4o Evaluation Results. Three metrics: Physical Realism (Physical), Photorealism (Photo) and Semantic Consistency (Semantic).

Method	Physical \uparrow	Photo \uparrow	Semantic \uparrow
CogVideoX-5B	0.612	0.858	0.617
Wan2.2-5B	0.609	0.877	<u>0.630</u>
ForcePrompt	0.615	0.875	0.611
OmniPhysGS	<u>0.622</u>	0.723	0.402
PhysGen	0.547	0.808	0.550
PhysGen3D	0.621	<u>0.879</u>	0.589
Ours	0.627	0.885	0.636

utilize GPT-4o to score the generated videos along three aspects: physical realism, photorealism, and semantic alignment with the textual prompt.

4.2. Comparisons with State-Of-The-Art Methods

Physics plausibility comparison. We aim to generate physically plausible, high-quality videos with consistent object motion and realistic interactions with the background. We compare our method with existing approaches on our constructed evaluation dataset. Quantitatively, as shown in Table 1, our method achieves superior motion coherence, consistently outperforming prior video generative models and showing comparable results with physical-engine-based methods across key dynamic metrics. Moreover, the generated videos exhibit higher visual quality than physical-engine-based methods. Regarding physical plausibility, as demonstrated in Table 2, our method surpasses all competing approaches on the physics realism metric, while simultaneously maintaining strong alignment with the input text, thereby ensuring high semantic consistency. Fig. 5 shows two qualitative comparisons. Existing methods suffer from texture degradation, incorrect motion dynamics, or inconsistent object-background interactions, often leading to object replacement. In contrast, our method consistently generates physically plausible and coherent object motion. More comparisons can be found in Appendix Sec. D.

Table 3. Evaluation of foreground multi-view video synthesis. **Bold**: Best. Underline: Second Best.

Method	View1			View2		
	Motion \uparrow	Subject \uparrow	Image \uparrow	Motion \uparrow	Subject \uparrow	Image \uparrow
DG4D	<u>0.986</u>	0.892	0.268	0.987	0.883	0.260
Diffusion ²	0.970	0.637	<u>0.371</u>	0.979	0.666	<u>0.362</u>
L4GM	0.994	<u>0.898</u>	0.368	<u>0.992</u>	<u>0.899</u>	0.305
Ours	0.995	0.912	0.389	0.994	0.901	0.368

Physical 4D quality comparison. We propose a two-stage framework that first generates multi-view foreground videos and then synthesizes the final video. To evaluate the quality of the generated orthogonal videos, we compare our method with existing 4D generation approaches, including DG4D (Ren et al., 2023), Diffusion² (Yang et al., 2025a), and L4GM (Ren et al., 2024a). For quantitative evaluation, we adopt VBench metrics to assess video quality from different views. As shown in Table 3, our method outperforms the competing approaches in terms of both motion consistency and visual quality. For qualitative comparison, representative results are shown in Fig. 6. Our method generates motion that follows physical principles, whereas existing 4D generation methods often fail to do so. Moreover, our approach effectively captures multi-view structure, producing consistent results from novel viewpoints.

4.3. Ablation Study

We introduce a physics-aware multi-view generation framework and conduct ablation studies to verify the effectiveness of key components in Phys4View. Specifically, we incrementally incorporate physics-aware attention (Phys-Attn), geometry-enhanced cross-view attention (Cross-view Attn), and temporal attention (Temporal-Attn). We evaluate results using two VBench metrics, namely Motion and Image, together with a physical realism score by GPT-4o. As shown in Table 4, introducing physics-aware attention leads to a significant improvement in physical realism. Adding geometry-enhanced cross-view attention further enhances motion smoothness and image quality, while temporal atten-

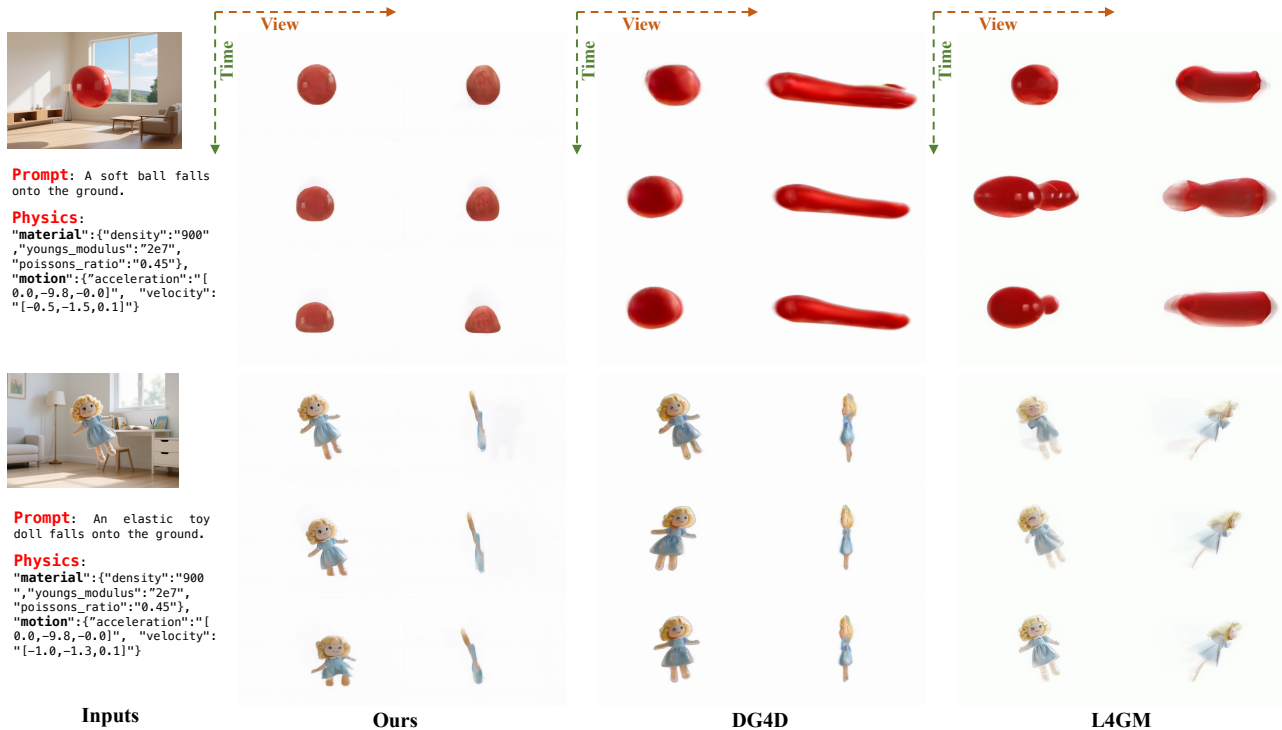


Figure 6. Qualitative comparison of multi-view video synthesis results. Each example includes the input image, prompt, and physics attributes, followed by synthesized videos rendered from two distinct views, illustrating temporal coherence and cross-view consistency.

Table 4. Ablation study of attention modules in Phys4View. The Motion and Image metrics are adopted from VBench, while the Physical metric is estimated using GPT-4o.

Method	Motion \uparrow	Image \uparrow	Physical \uparrow
Baseline*	0.994	0.594	0.636
+ Physics-Attn	0.994	0.613	0.682
+ Cross-View Attn	0.995	0.648	0.689
+ Temporal-Attn	0.996	0.655	0.691

tion provides additional gains in motion consistency. The qualitative ablation comparison is shown in Appendix Fig. 8. Additional ablation study on condition videos is detailed in Appendix Fig. 9.

5. Downstream Applications

While our primary focus is video generation rather than full 4D modeling, the orthogonal four-view foreground videos produced by our method naturally enable several downstream applications. As a demonstration, we show that the generated four-view foreground videos are well-suited for video editing. As illustrated in Fig. 7, we modify the rotation of the foreground object and leverage the foreground video segment from one of the generated views to guide the synthesis of an edited video. Additionally, although not a central goal of our method, for scenes with simple backgrounds, our approach can generate four-view videos with background, producing spatially consistent foreground-background ren-



Figure 7. Results of object editing. The top row shows the original results, and the bottom row shows edited videos with the object rotated by 90°, maintaining multi-view consistency.

derings across views, as shown in Appendix Fig. 11.

6. Conclusion

In this work, we propose PhysVideo, a physics-driven framework for geometry-aware motion modeling in video generation. PhysVideo introduces physics-aware and geometry-enhanced inductive biases to improve motion consistency and physical plausibility without relying on explicit 3D representation. The framework combines physics-conditioned multi-view motion modeling with background-aware video synthesis, enabling controllable video generation. Extensive experiments demonstrate that PhysVideo achieves superior motion coherence, visual quality, and physical realism compared to existing methods. In addition, we introduce a large-scale physics-oriented multi-view video dataset to facilitate future research.

Impact Statement

This paper presents work whose goal is to advance the field of machine learning, with a focus on physically plausible video generation. There are many potential societal consequences of this work, none of which we feel must be specifically highlighted here.

References

- Bansal, H., Lin, Z., Xie, T., Zong, Z., Yarom, M., Bitton, Y., Jiang, C., Sun, Y., Chang, K.-W., and Grover, A. Videophy: Evaluating physical commonsense for video generation. *arXiv preprint arXiv:2406.03520*, 2024.
- Blattmann, A., Dockhorn, T., Kulal, S., Mendeleevitch, D., Kilian, M., Lorenz, D., Levi, Y., English, Z., Voleti, V., Letts, A., et al. Stable video diffusion: Scaling latent video diffusion models to large datasets. *arXiv preprint arXiv:2311.15127*, 2023.
- Burgert, R., Xu, Y., Xian, W., Pilarski, O., Clausen, P., He, M., Ma, L., Deng, Y., Li, L., Mousavi, M., et al. Go-with-the-flow: Motion-controllable video diffusion models using real-time warped noise. In *Proceedings of the Computer Vision and Pattern Recognition Conference*, pp. 13–23, 2025.
- Chen, B., Jiang, H., Liu, S., Gupta, S., Li, Y., Zhao, H., and Wang, S. Physgen3d: Crafting a miniature interactive world from a single image. In *Proceedings of the Computer Vision and Pattern Recognition Conference*, pp. 6178–6189, 2025a.
- Chen, Z., Xu, T., Wu, L., Wang, L., Yan, D., You, Z., Luo, W., Zhang, G., and Chen, Y. Stance: Motion coherent video generation via sparse-to-dense anchored encoding. *arXiv preprint arXiv:2510.14588*, 2025b.
- Dong, Q. and Fu, Y. Memflow: Optical flow estimation and prediction with memory. In *Proceedings of the IEEE/CVF Conference on Computer Vision and Pattern Recognition*, pp. 19068–19078, 2024.
- Duan, H., Yu, H.-X., Chen, S., Fei-Fei, L., and Wu, J. World-score: A unified evaluation benchmark for world generation. *arXiv preprint arXiv:2504.00983*, 2025.
- Feng, Y., Feng, X., Shang, Y., Jiang, Y., Yu, C., Zong, Z., Shao, T., Wu, H., Zhou, K., Jiang, C., et al. Gaussian splashing: Dynamic fluid synthesis with gaussian splatting. *CoRR*, 2024.
- Fu, X., Liu, X., Wang, X., Peng, S., Xia, M., Shi, X., Yuan, Z., Wan, P., Zhang, D., and Lin, D. 3dtrajmaster: Mastering 3d trajectory for multi-entity motion in video generation. *arXiv preprint arXiv:2412.07759*, 2024.
- Gao, Y., Yu, H.-X., Zhu, B., and Wu, J. Fluidnexus: 3d fluid reconstruction and prediction from a single video. In *Proceedings of the Computer Vision and Pattern Recognition Conference*, pp. 26091–26101, 2025.
- Geng, D., Herrmann, C., Hur, J., Cole, F., Zhang, S., Pfaff, T., Lopez-Guevara, T., Aytar, Y., Rubinstein, M., Sun, C., et al. Motion prompting: Controlling video generation with motion trajectories. In *Proceedings of the Computer Vision and Pattern Recognition Conference*, pp. 1–12, 2025.
- Gillman, N., Herrmann, C., Freeman, M., Aggarwal, D., Luo, E., Sun, D., and Sun, C. Force prompting: Video generation models can learn and generalize physics-based control signals. *arXiv preprint arXiv:2505.19386*, 2025.
- Gu, Z., Yan, R., Lu, J., Li, P., Dou, Z., Si, C., Dong, Z., Liu, Q., Lin, C., Liu, Z., et al. Diffusion as shader: 3d-aware video diffusion for versatile video generation control. In *Proceedings of the Special Interest Group on Computer Graphics and Interactive Techniques Conference Conference Papers*, pp. 1–12, 2025.
- He, H., Xu, Y., Guo, Y., Wetzstein, G., Dai, B., Li, H., and Yang, C. Cameractrl: Enabling camera control for text-to-video generation. *arXiv preprint arXiv:2404.02101*, 2024.
- Ho, J., Salimans, T., Gritsenko, A., Chan, W., Norouzi, M., and Fleet, D. J. Video diffusion models. *Advances in neural information processing systems*, 35:8633–8646, 2022.
- Hu, Y., Li, T.-M., Anderson, L., Ragan-Kelley, J., and Durand, F. Taichi: a language for high-performance computation on spatially sparse data structures. *ACM Transactions on Graphics (TOG)*, pp. 1–16, 2019.
- Huang, T., Zhang, H., Zeng, Y., Zhang, Z., Li, H., Zuo, W., and Lau, R. W. Dreamphysics: Learning physics-based 3d dynamics with video diffusion priors. In *Proceedings of the AAAI Conference on Artificial Intelligence*, pp. 3733–3741, 2025.
- Huang, Z., He, Y., Yu, J., Zhang, F., Si, C., Jiang, Y., Zhang, Y., Wu, T., Jin, Q., Chanpaisit, N., et al. Vbench: Comprehensive benchmark suite for video generative models. In *Proceedings of the IEEE/CVF Conference on Computer Vision and Pattern Recognition*, pp. 21807–21818, 2024.
- Jin, W., Dai, Q., Luo, C., Baek, S.-H., and Cho, S. Flovd: Optical flow meets video diffusion model for enhanced camera-controlled video synthesis. In *Proceedings of the Computer Vision and Pattern Recognition Conference*, pp. 2040–2049, 2025.

- Kerbl, B., Kopanas, G., Leimkühler, T., and Drettakis, G. 3d gaussian splatting for real-time radiance field rendering. *ACM Trans. Graph.*, 42(4):139–1, 2023.
- Kong, W., Tian, Q., Zhang, Z., Min, R., Dai, Z., Zhou, J., Xiong, J., Li, X., Wu, B., Zhang, J., et al. Hunyuan-video: A systematic framework for large video generative models. *arXiv preprint arXiv:2412.03603*, 2024.
- Langley, P. Crafting papers on machine learning. In Langley, P. (ed.), *Proceedings of the 17th International Conference on Machine Learning (ICML 2000)*, pp. 1207–1216, Stanford, CA, 2000. Morgan Kaufmann.
- Li, Z., Tucker, R., Snavely, N., and Holynski, A. Generative image dynamics. In *Proceedings of the IEEE/CVF Conference on Computer Vision and Pattern Recognition*, pp. 24142–24153, 2024.
- Liang, F., Wu, B., Wang, J., Yu, L., Li, K., Zhao, Y., Misra, I., Huang, J.-B., Zhang, P., Vajda, P., et al. Flowvid: Taming imperfect optical flows for consistent video-to-video synthesis. In *Proceedings of the IEEE/CVF Conference on Computer Vision and Pattern Recognition*, pp. 8207–8216, 2024.
- Lin, J., Wang, Z., Xu, D., Jiang, S., Gong, Y., and Jiang, M. Phys4dgen: Physics-compliant 4d generation with multi-material composition perception. In *Proceedings of the 33rd ACM International Conference on Multimedia*, pp. 10398–10407, 2025a.
- Lin, Y., Lin, C., Xu, J., and Mu, Y. Omniphysgs: 3d constitutive gaussians for general physics-based dynamics generation. *arXiv preprint arXiv:2501.18982*, 2025b.
- Liu, F., Wang, H., Yao, S., Zhang, S., Zhou, J., and Duan, Y. Physics3d: Learning physical properties of 3d gaussians via video diffusion. *arXiv preprint arXiv:2406.04338*, 2024a.
- Liu, S., Ren, Z., Gupta, S., and Wang, S. Physgen: Rigid-body physics-grounded image-to-video generation. In *European Conference on Computer Vision*, pp. 360–378, 2024b.
- Lv, J., Huang, Y., Yan, M., Huang, J., Liu, J., Liu, Y., Wen, Y., Chen, X., and Chen, S. Gpt4motion: Scripting physical motions in text-to-video generation via blender-oriented gpt planning. In *Proceedings of the IEEE/CVF conference on computer vision and pattern recognition*, pp. 1430–1440, 2024.
- Mao, H., Xu, Z., Wei, S., Quan, Y., Deng, N., and Yang, X. Live-gs: Llm powers interactive vr by enhancing gaussian splatting. In *2025 IEEE Conference on Virtual Reality and 3D User Interfaces Abstracts and Workshops (VRW)*, pp. 1234–1235. IEEE, 2025.
- Meng, F., Liao, J., Tan, X., Shao, W., Lu, Q., Zhang, K., Cheng, Y., Li, D., Qiao, Y., and Luo, P. Towards world simulator: Crafting physical commonsense-based benchmark for video generation. *arXiv preprint arXiv:2410.05363*, 2024.
- Nan, K., Xie, R., Zhou, P., Fan, T., Yang, Z., Chen, Z., Li, X., Yang, J., and Tai, Y. Openvid-1m: A large-scale high-quality dataset for text-to-video generation. *arXiv preprint arXiv:2407.02371*, 2024.
- Poole, B., Jain, A., Barron, J. T., and Mildenhall, B. Dreamfusion: Text-to-3d using 2d diffusion. *arXiv preprint arXiv:2209.14988*, 2022.
- Ren, J., Pan, L., Tang, J., Zhang, C., Cao, A., Zeng, G., and Liu, Z. Dreamgaussian4d: Generative 4d gaussian splatting. *arXiv preprint arXiv:2312.17142*, 2023.
- Ren, J., Xie, C., Mirzaei, A., Kreis, K., Liu, Z., Torralba, A., Fidler, S., Kim, S. W., Ling, H., et al. L4gm: Large 4d gaussian reconstruction model. *Advances in Neural Information Processing Systems*, 37:56828–56858, 2024a.
- Ren, T., Liu, S., Zeng, A., Lin, J., Li, K., Cao, H., Chen, J., Huang, X., Chen, Y., Yan, F., et al. Grounded sam: Assembling open-world models for diverse visual tasks. *arXiv preprint arXiv:2401.14159*, 2024b.
- Romero, D., Bermudez, A., Li, H., Pizzati, F., and Laptev, I. Learning to generate object interactions with physics-guided video diffusion. *arXiv preprint arXiv:2510.02284*, 2025.
- Wan, T., Wang, A., Ai, B., Wen, B., Mao, C., Xie, C.-W., Chen, D., Yu, F., Zhao, H., Yang, J., et al. Wan: Open and advanced large-scale video generative models. *arXiv preprint arXiv:2503.20314*, 2025.
- Wang, J., Ma, A., Cao, K., Zheng, J., Zhang, Z., Feng, J., Liu, S., Ma, Y., Cheng, B., Leng, D., et al. Wisa: World simulator assistant for physics-aware text-to-video generation. *arXiv preprint arXiv:2503.08153*, 2025.
- Wu, C., Li, J., Zhou, J., Lin, J., Gao, K., Yan, K., Yin, S.-m., Bai, S., Xu, X., Chen, Y., et al. Qwen-image technical report. *arXiv preprint arXiv:2508.02324*, 2025.
- Wu, G., Tao, X., Li, C., Wang, W., Liu, X., and Zheng, Q. Perception-oriented video frame interpolation via asymmetric blending. In *Proceedings of the IEEE/CVF Conference on Computer Vision and Pattern Recognition*, pp. 2753–2762, 2024.
- Xiang, J., Lv, Z., Xu, S., Deng, Y., Wang, R., Zhang, B., Chen, D., Tong, X., and Yang, J. Structured 3d latents for scalable and versatile 3d generation. In *Proceedings of the Computer Vision and Pattern Recognition Conference*, pp. 21469–21480, 2025.

- Xie, T., Zong, Z., Qiu, Y., Li, X., Feng, Y., Yang, Y., and Jiang, C. Physgaussian: Physics-integrated 3d gaussians for generative dynamics. In *Proceedings of the IEEE/CVF Conference on Computer Vision and Pattern Recognition*, pp. 4389–4398, 2024.
- Xue, Q., Yin, X., Yang, B., and Gao, W. Phyt2v: Llm-guided iterative self-refinement for physics-grounded text-to-video generation. In *Proceedings of the Computer Vision and Pattern Recognition Conference*, pp. 18826–18836, 2025.
- Yang, L., Kang, B., Huang, Z., Zhao, Z., Xu, X., Feng, J., and Zhao, H. Depth anything v2. *Advances in Neural Information Processing Systems*, 37:21875–21911, 2024.
- Yang, Z., Pan, Z., Gu, C., and Zhang, L. Diffusion²: Dynamic 3d content generation via score composition of video and multi-view diffusion models. In *International Conference on Learning Representations (ICLR)*, 2025a.
- Yang, Z., Teng, J., Zheng, W., Ding, M., Huang, S., Xu, J., Yang, Y., Hong, W., Zhang, X., Feng, G., et al. Cogvideox: Text-to-video diffusion models with an expert transformer. In *The Thirteenth International Conference on Learning Representations*, 2025b.
- Zhang, T., Yu, H.-X., Wu, R., Feng, B. Y., Zheng, C., Snavely, N., Wu, J., and Freeman, W. T. Physdreamer: Physics-based interaction with 3d objects via video generation. In *European Conference on Computer Vision*, pp. 388–406, 2024.
- Zhao, H., Wang, H., Zhao, X., Fei, H., Wang, H., Long, C., and Zou, H. Physsplat: Efficient physics simulation for 3d scenes via mllm-guided gaussian splatting. In *Proceedings of the IEEE/CVF International Conference on Computer Vision*, pp. 5242–5252, 2025.
- Zheng, Z., Peng, X., Yang, T., Shen, C., Li, S., Liu, H., Zhou, Y., Li, T., and You, Y. Open-sora: Democratizing efficient video production for all. *arXiv preprint arXiv:2412.20404*, 2024.

Appendix

A. Additional Experiments

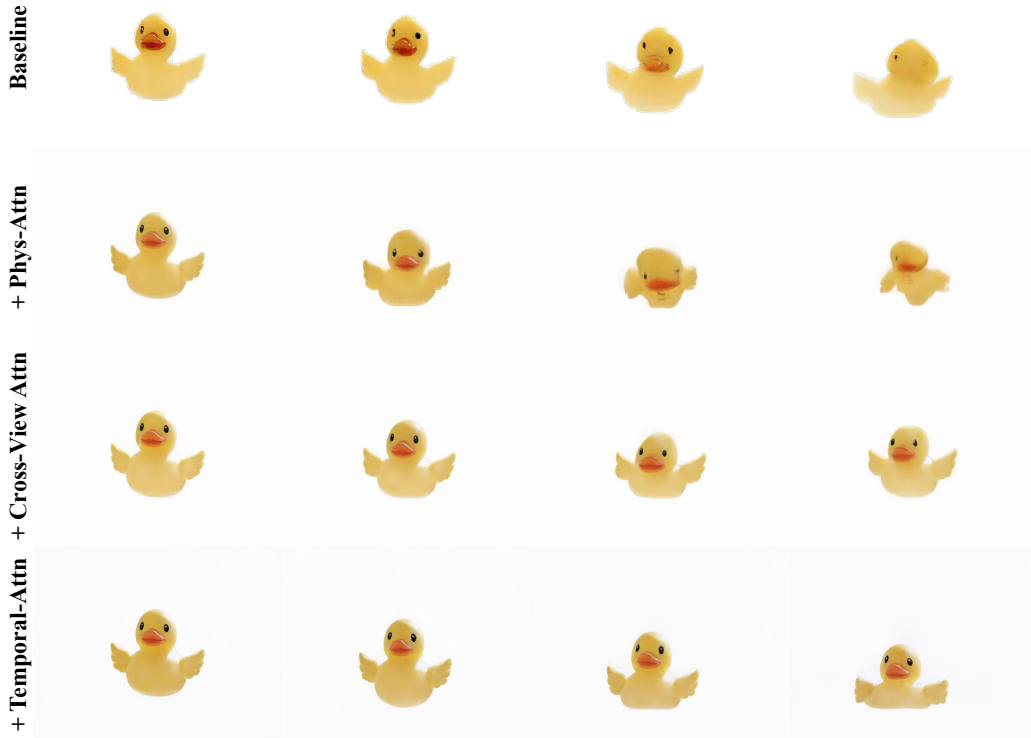


Figure 8. **Qualitative ablation results.** We compare the baseline with variants that incorporate individual components, including Phys-Attn, Cross-View Attn, and Temporal-Attn. Each row corresponds to one setting.

A.1. Ablation Study of Attention Modules.

In the main manuscript, we report quantitative ablation results in Table 4 to evaluate the contribution of different attention modules. Here, we further provide qualitative ablation results in Fig. 8 to offer visual insights into their effects on orthogonal foreground video generation. As shown in Fig. 8, progressively introducing physics-aware attention, geometry-enhanced cross-view attention, and temporal attention leads to more coherent motion patterns and improved visual quality. These qualitative results complement the quantitative analysis and further validate the effectiveness of each proposed component.

A.2. Ablation Study of Condition Videos.

We employ two types of video conditions to guide the four-view generation process. To evaluate the effectiveness of these conditions, we conduct an ablation study with qualitative comparisons shown in Fig. 9. The foreground mask video condition provides explicit guidance for foreground object motion, while the multi-view video condition implicitly encodes 3D structural information, leading to more spatially consistent four-view video generation.

A.3. Evaluation with GPT-4o.

Since no widely accepted, physics-focused evaluation metrics for image-to-video generation currently exist, we follow the approach of PhysGen3D (Chen et al., 2025a) and employ GPT-4o to conduct subjective assessments. These evaluations score multiple dimensions relevant to physical plausibility, including physical realism, photorealism, and semantic alignment. We adopt the evaluation prompt design originally proposed in PhysGen3D (Chen et al., 2025a); as their work has empirically demonstrated strong alignment with human judgment, we apply only minor adaptations to tailor the prompt to our dataset,

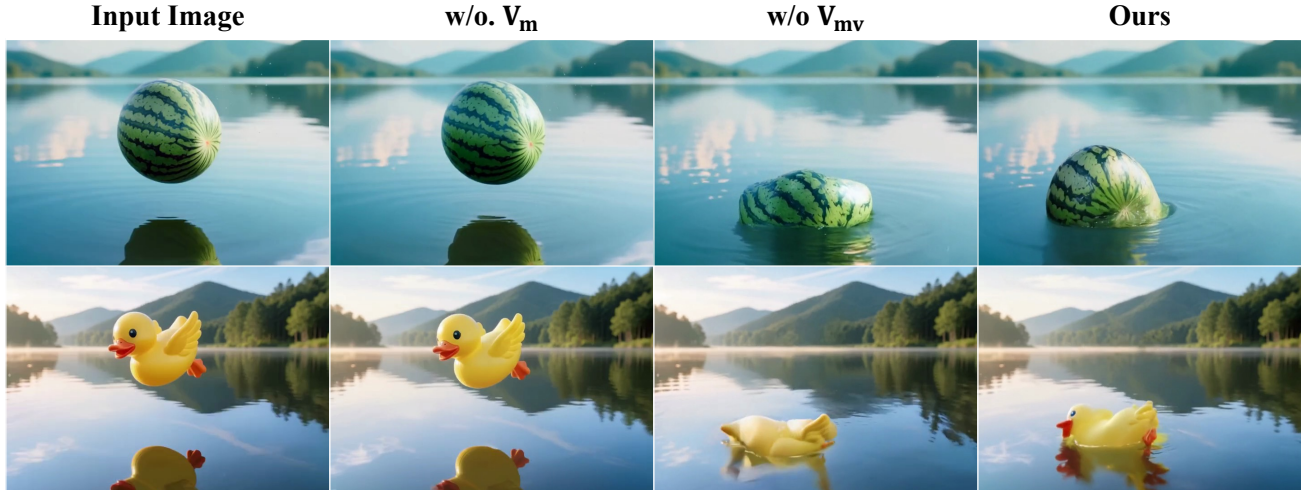


Figure 9. **Ablation study on conditional videos.** The left column shows the input single image, and the three right columns each display one representative frame from the generated RGB video.

without introducing substantial modifications. The complete evaluation prompt is illustrated in Fig. 10.

B. Application of 4D Synthesis

Our method not only supports object editing while preserving a stable background, but also enables four-view video generation with simple backgrounds. As shown in Fig. 11, we render four-view videos from the front, left, back, and right viewpoints. The generated results exhibit strong cross-view consistency, and the interactions between foreground objects and background remain visually plausible.

C. Details of PhysMV Dataset

In the main manuscript, we introduce the PhysMV dataset. Here we provide further detailed information. We generate 10K 3D objects and reconstruct 10 diverse background scenes, each represented by a 3D-GS model that supports viewpoint exploration. Following the design of OmniPhysGS (Lin et al., 2025b), we employ TaiChi (Hu et al., 2019) as the physics engine and adopt the Material Point Method (MPM) as the physics solver to simulate object dynamics conditioned on the specified physical properties. Leveraging the rendering capability of 3D-GS, we render four-view foreground videos after the physical simulation. Note that the generated four-view videos contain only foreground objects, as the background scenes do not support full 360-degree rendering across all views. The dataset examples are shown in Fig. 12.

For each simulated sample, the textual prompt, motion attributes, and material parameters used to control the physics simulation are automatically recorded as metadata. During post-processing, we apply Grounded-SAM (Ren et al., 2024b) to obtain semantic foreground masks and DepthAnything V2 (Yang et al., 2024) to get relative depth maps. Finally, Trellis (Xiang et al., 2025) is again utilized to generate multi-view videos of the segmented foreground objects, which are used to provide multi-view video priors.

D. More Visual Comparisons with Baselines

As shown in Fig. 13, Fig. 14, Fig. 15, and Fig. 16, we provide additional visual comparisons with all baseline methods. These results highlight that our method achieves state-of-the-art quality, characterized by high visual fidelity, strong physical plausibility, and fine-grained controllability.

System Prompt

You are a helpful assistant that pays attention to context and estimates the perceptual quality of a video based on physical realism, photorealism, and semantic consistency.

User Prompt

I would like you to evaluate the quality of generated videos based on the following criteria: physical realism, photorealism, and semantic consistency. The evaluation will be based on 15 evenly sampled frames from each video. Given the following instructions: '{instructions}', please evaluate the quality of each video on the three criteria mentioned above. And for the definition of velocity and acceleration directions, the positive x-axis is defined as horizontal left, the positive y-axis as vertical upward, and the positive z-axis as perpendicular to the paper plane inward.

Note that: **Physical realism** focuses on input-conditioned physical fidelity: the object's motion and deformation must be consistent with the physical properties specified in the input (e.g., motion direction and deformation magnitude). Any noticeable mismatch with the provided physical attributes should be considered a degradation in physical realism. **Photorealism** assesses the overall visual quality of the video, including the presence of visual artifacts, discontinuities, and how accurately the video replicates details of light, texture, and materials. **Semantic Consistency** evaluates how well the content of the generated video aligns with the intended meaning of the text prompt.

Please provide scores from 0-1, with 1 being the best. The output must follow this exact format: Physical Realism Score: [a score]; Photorealism Score: [a score]; Semantic Consistency Score: [a score]

Note that your output should strictly follow the above format, with a ';' after each score. Do not give any other explanations.

Figure 10. Prompt used for GPT-4o evaluation.

E. Limitations and Future Work

While our method introduces a novel framework for generating physics-aware 4D foreground video with background interaction from a given viewpoint, it still exhibits several limitations. In particular, our approach is currently constrained in its ability to model and synthesize complex and highly dynamic backgrounds. Although the proposed method can generate diverse and physically plausible 4D foreground motions, synthesizing complete videos from novel viewpoints remains challenging when the background contains rich geometric structures or intricate appearance variations. This limitation primarily stems from the inherent difficulty of holistic scene modeling, which has not yet been fully addressed by existing 3D generation and reconstruction methods, and becomes even more challenging in the 4D setting where temporal dynamics must be consistently preserved. As a result, background reconstruction quality may degrade when extrapolating to unseen viewpoints, which in turn affects the overall visual coherence of the generated video.

In future work, we plan to explore more advanced scene representations and background modeling strategies to better capture complex geometry and long-range temporal consistency. Integrating explicit scene decomposition, multi-view supervision, or hybrid 3D-4D representations may help alleviate these limitations and enable more robust whole-scene generation from novel viewpoints.

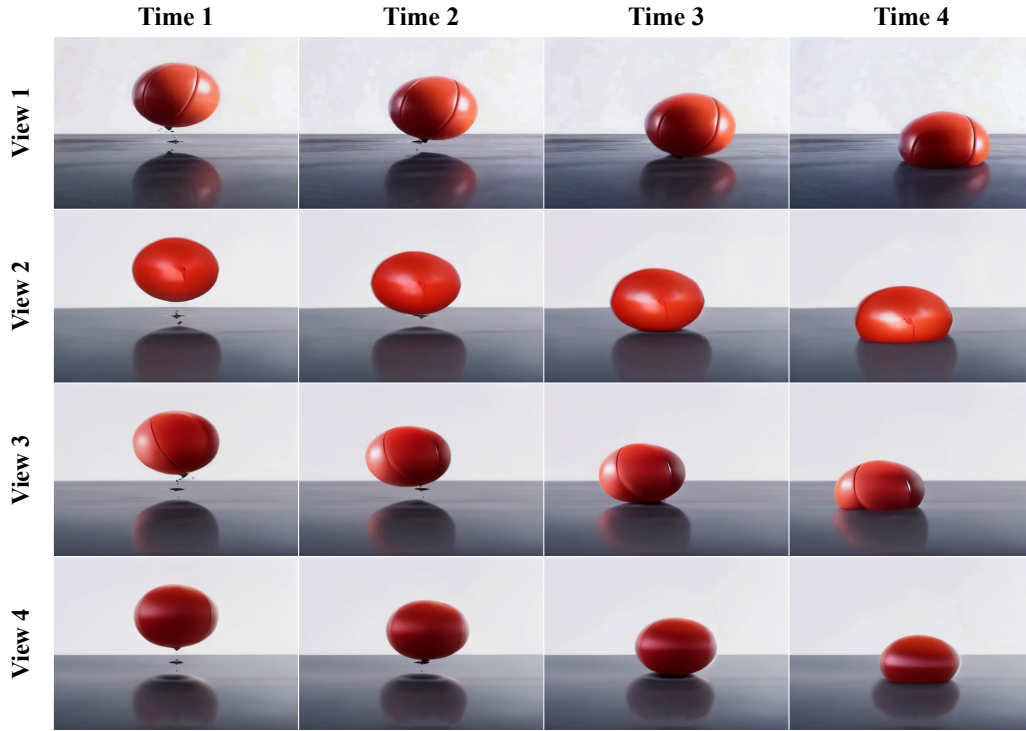


Figure 11. Four-view video generation results. Views 1 through 4 correspond to the front, left, rear, and right viewpoints, respectively.

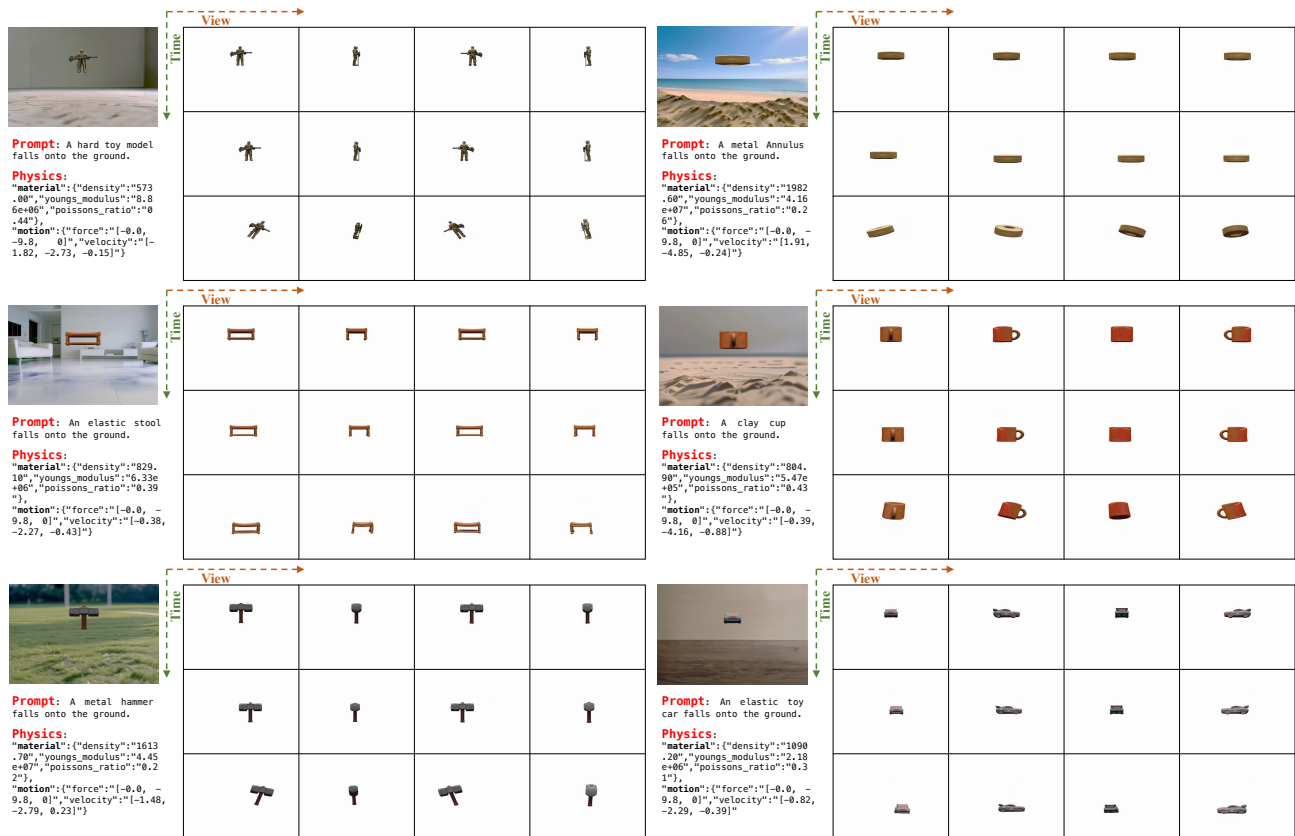


Figure 12. Dataset demonstration. Our dataset contains various objects and motion patterns.

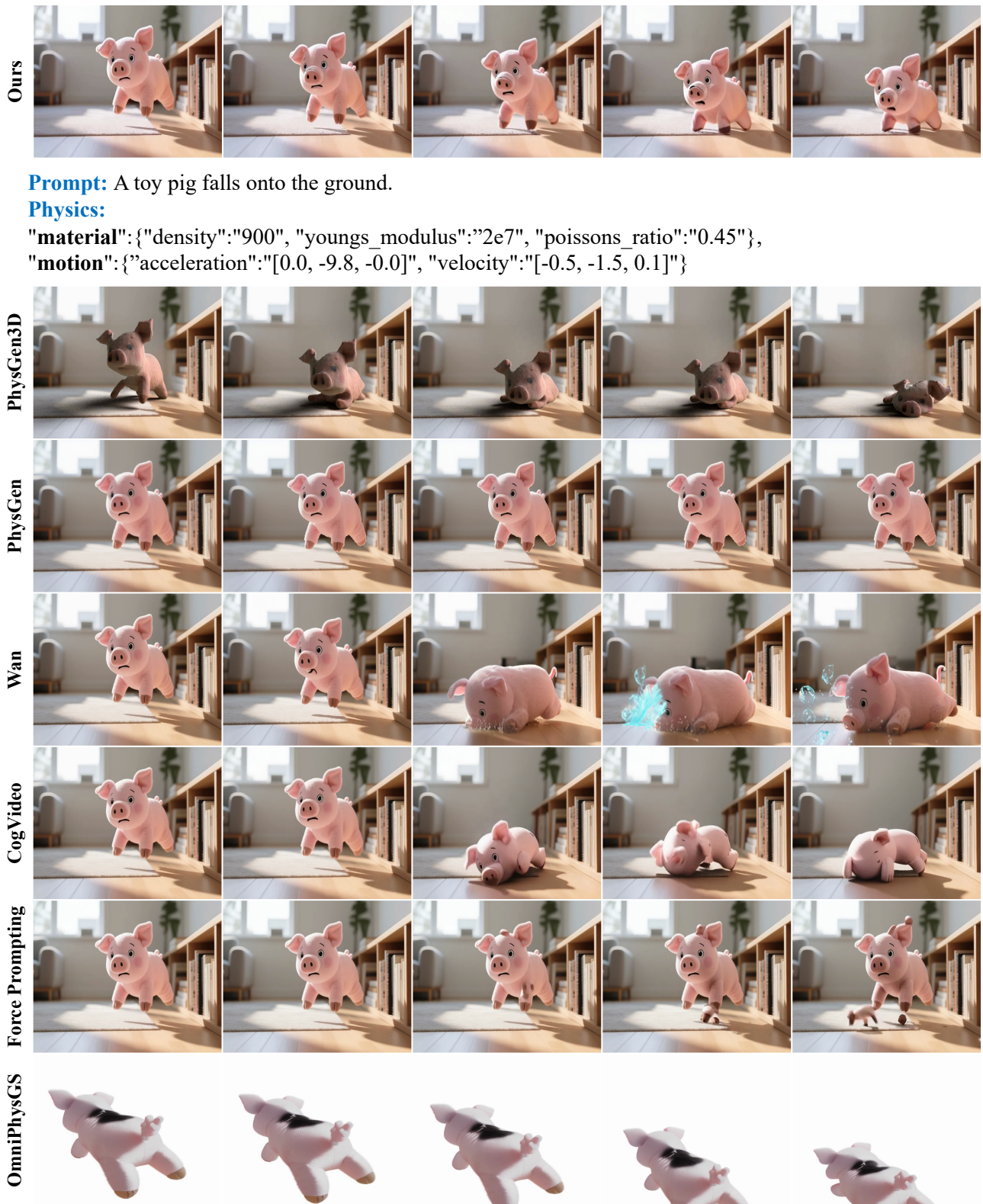


Figure 13. Qualitative visualization results of our method and the baselines.



Figure 14. Qualitative visualization results of our method and the baselines.

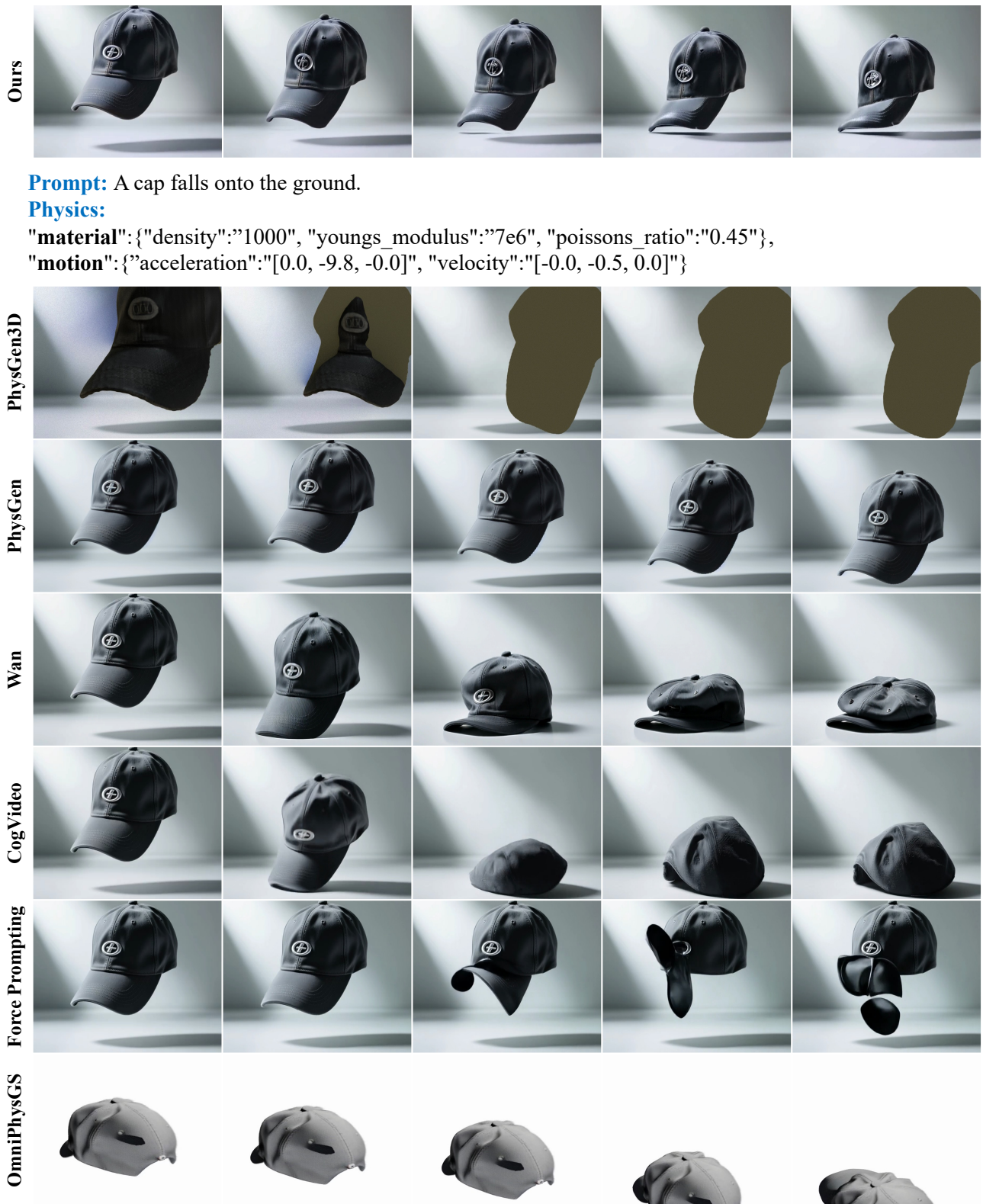


Figure 15. Qualitative visualization results of our method and the baselines.

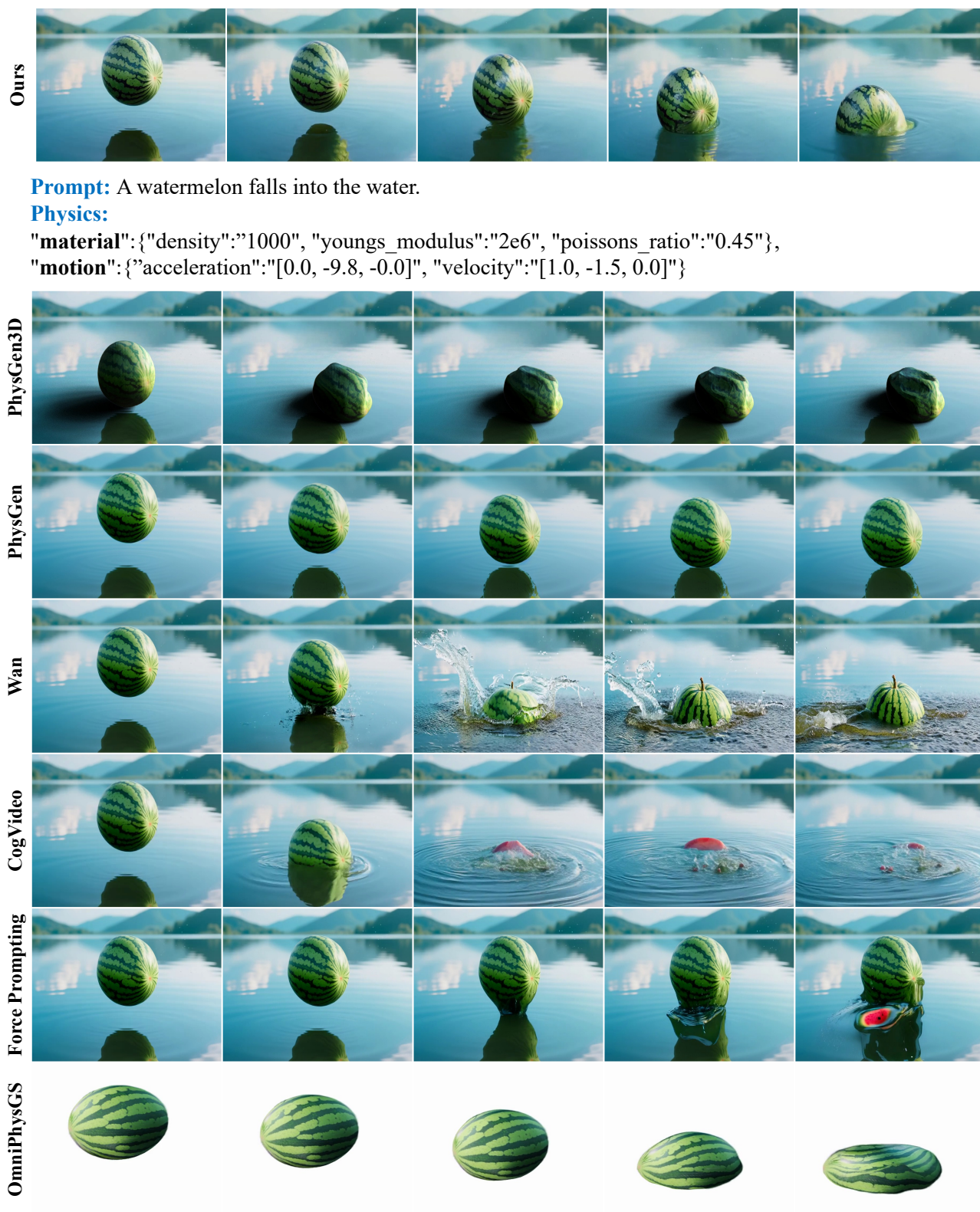


Figure 16. Qualitative visualization results of our method and the baselines.